J. Fluid Mech. (1992), *vol.* 234, *pp.* 473–486
Printed in Great Britain

Self-similar spin-up and spin-down in a cylinder of small ratio of height to diameter

By F. V. DOLZHANSKII, V. A. KRYMOV AND D. YU. MANIN
Institute of Atmospheric Physics, 3, Pyzhevsky, Moscow, 109017, USSR

(Received 22 June 1990 and in revised form 15 July 1991)

A new approach to the well-known spin-up from rest problem is proposed based on a search for self-similarity. The Wedemeyer (1963) model is first tested for spin-down to rest and then used for spin-up. The general-form solution is found and is shown to tend to a self-similar limiting stage. Experimental results in a cylinder of small height-to-diameter ratio are analysed to demonstrate this self-similarity in a certain range of external parameters.

1. Introduction

The present study deals with the spin-up problem, i.e. the process of the fluid angular velocity ω adjustment to the impulsive change of the cylindrical container rotation rate. The external parameters controlling the process are the fluid viscosity ν, the height H, and radius R of the cylinder, the initial angular velocity of the cylinder Ω, and its increment $\Delta\Omega$. We assume the fluid to be incompressible and homogeneous. Spin-up from rest ($\Omega = 0, \Delta\Omega > 0$) is considered in this paper.

The definitive paper by Greenspan & Howard (1963) revealed the basic mechanism underlying the spin-up process. They considered the case of a fluid confined between two infinite plates ($R = \infty$). Under the assumption that Ekman and Rossby numbers are both small, $E = \nu/\Omega H^2 \ll 1$, $\epsilon = \Delta\Omega/\Omega \ll 1$ respectively, they were able to obtain an asymptotic solution. The solution shows that the timescale of spin-up is $\tau_E = H/(\Omega\nu)^{\frac{1}{2}}$, which is much greater than the Ekman layer timescale $\tau_\Omega = \Omega^{-1}$ and much less than the viscous timescale $\tau_\nu = H^2/\nu$.

The effect of the sidewall is negligible in the linear ($\epsilon \ll 1$), inviscid ($E \ll 1$) case. In fact, the sidewall can influence the flow only in the thin Proudman–Stewartson $E^{\frac{1}{4}}$-layer (Proudman 1956; Stewartson 1957; Greenspan 1968), via both viscous diffusion and advection of momentum. This is not the case when the Rossby number is no longer small, when nonlinear effects become important and one should distinguish between spin-up and spin-down (which is unnecessary in the linear case). The presence of the sidewall should also be taken into account.

Greenspan & Weinbaum (1963) and Benton (1973) extended the method of Greenspan & Howard (1963) to the weakly nonlinear case (up to the terms of order ϵ^2). They found that nonlinearity would slightly decrease the characteristic time of spin-down and increase that of spin-up. Weidman (1976*a*, *b*) conjectured that an algebraic, rather than exponential, dependence of the azimuthal velocity on time, $v \propto t^{-2}$, is likely for the spin-down to rest between infinite plates. This can be easily understood if we write $\dot{\omega} \sim \omega/\tau_E$, $\tau_E = H/(\omega\nu)^{\frac{1}{2}}$ being the current Ekman timescale. This gives $\dot{\omega} \sim \omega^{\frac{3}{2}}$, whence $\omega \sim t^{-2}$.

The sidewall instabilities, however, can make the fluid motion become turbulent in spin-down (cf. Mathis & Neitzel 1985), which prevented Weidman (1976*a*, *b*) from

experimentally verifying the dependence $\omega \sim t^{-2}$. This problem can be eliminated (Krymov & Manin 1986*a*, hereinafter referred to as K&M*a*) by using a cylinder with $R \gg H$. The experimental data obtained there are in good agreement with theoretical predictions. In addition, the case of spin-down with a non-solid-rotation initial conditions was considered theoretically and a class of self-similar solutions was found. In Krymov & Manin (1986*b*, hereinafter K&M*b*) the self-similar spin-down was observed experimentally in a space between two cones.

Another branch of the spin-up problem, namely spin-up from rest, originated from the work of Wedemeyer (1964), who constructed a semi-empirical equation based on the assumption that the boundary layers are of the Kármán type (Greenspan 1968). This equation is obtained from an equation for the internal region (beyond the boundary layers) for the case of small Ekman number, which can be written down in dimensionless form as

$$\frac{\partial v}{\partial t}+E^{-\frac{1}{2}}u\left(\frac{\partial v}{\partial r}+\frac{v}{r}\right)=E^{\frac{1}{2}}\frac{H^2}{R^2}\left(\frac{\partial^2 v}{\partial r^2}+\frac{\partial}{\partial r}\frac{v}{r}\right).$$

Here v is the azimuthal velocity and u is the radial velocity. Radius r is normalized by R, time t by τ_{E} and velocity by ΩR. Upon expressing u in terms of v via the Ekman suction condition $u = \kappa E^{\frac{1}{2}}(v-r)$ (for spin-up), where κ is a constant of the order of unity, the equation takes the closed form

$$\frac{\partial v}{\partial t}+\kappa(v-r)\left(\frac{\partial v}{\partial r}+\frac{v}{r}\right)=E^{\frac{1}{2}}\frac{H^2}{R^2}\left(\frac{\partial^2 v}{\partial r^2}+\frac{\partial}{\partial r}\frac{v}{r}\right). \tag{1}$$

Note that the dimensionless parameter $E^{\frac{1}{2}}H^2/R^2$ can be interpreted as the squared ratio of the Proudman–Stewartson $E^{\frac{1}{4}}$ layer width over the radius of the container. It is defined in a similar manner as the Ekman number (which is the squared ratio of the Ekman layer width over the depth of the fluid), so we shall call it the Stewartson number

$$St = E^{\frac{1}{2}}H^2/R^2 = \delta_{\mathrm{S}}^2/R^2 = H\nu^{\frac{1}{2}}/R^2\Omega^{\frac{1}{2}}. \tag{2}$$

By neglecting the radial viscous term Wedemeyer obtained a solution which describes the fluid acceleration during spin-up. According to this solution the fluid is sucked into Ekman layers and accelerated there towards the sidewall. Then, pushed into the internal region, it takes the place of the as yet non-rotating fluid. The characteristic time of spin-up from rest is again of the order τ_{E}. An important feature of the process is the existence of a vertical layer dividing the rotating and non-rotating fluid. It originates at the sidewall and propagates inwards, being clearly visible via the aluminium powder technique (Savaş 1985). Venezian (1969) showed that this layer is actually the propagating Stewartson $E^{\frac{1}{4}}$-layer.

Though qualitative agreement with the Wedemeyer solution is clear, quantitative agreement with laboratory or numerical experiment was never achieved. The efforts of different workers were aimed mainly at the improvement of the Wedemeyer model by taking account of the radial viscosity (Venezian 1969; Watkins & Hussey 1973, 1977; Kitchens 1980) or by modifying the Ekman pumping condition (Weidman 1976*a*, *b*; Benton 1979; Kitchens 1980). In the present work another approach is proposed.

We note, first of all, that the only external parameter in the Wedemeyer equation (1), namely the Stewartson number St, depends on R much more strongly than on Ω. So in order to achieve small St values it is preferable to increase R rather than Ω (provided that Ω is already large enough for the Ekman number to be small). This leads again to the concept of a cylinder of small ratio of height to diameter.

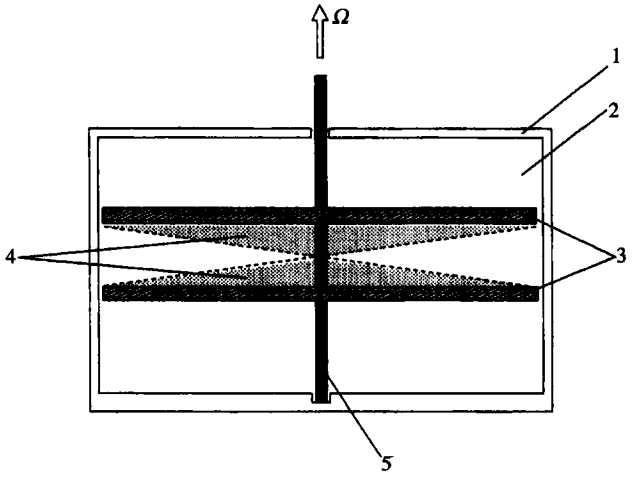

FIGURE 1. Experimental apparatus. 1, Plexiglas cube with a cylindrical cavity, 2, in it; 3, two flat disks (or cones, 4, interchangeable with disks); 5, vertical axis.

Secondly, Wedemeyer and successors posed the boundary condition of constant angular velocity at the sidewall and considered the flow to be laminar. However, Weidman (1976*a*, *b*) observed turbulence in the vicinity of the sidewall at the initial stage of spin-up. The turbulence soon decays and a laminar initial state forms and develops. So it seems to be more appropriate to solve an initial-value problem rather than a boundary-value one (even in view of a certain vagueness of the initial state). In the present study experiments were conducted in a container with a non-rotating sidewall, which makes the boundary-value formulation even less appropriate. Nevertheless, this does not affect the flow far from the sidewall. The reproducibility and accordance with previous results allows to presume that the initial-value solution for spin-up tends to a unique limiting stage insensitive to the details of the initial state.

The present paper is organized as follows. First we describe the experimental set-up common for K&M(*a*, *b*) and this work. Next the principal results of K&M are reviewed in order to check the applicability of the Wedemeyer equation. Then the general-form solution of the Wedemeyer equation for spin-up is derived and it is shown to tend to a self-similar limiting case. Experimental results are described and compared with theory.

2. Experimental set-up

The laboratory apparatus (figure 1) consisted of a Plexiglas cube, 1, with a cylindrical cavity, 2, in it. Two flat disks, 3, (or cones, 4, with half-angle $\theta_0 = 78.7°$, $\cot\theta_0 = \frac{1}{5}$) of radius $R = 10$ cm were mounted in the cavity on a vertical axis, 5, of radius $R_0 = 0.3$ cm. (Note that cones were used in spin-down experiments only.) The gap between the edges of the disks and the inside wall of the cavity did not exceed 0.05 cm. The distance H between disks ranged from 0.7 to 2.0 cm. The rotation rate of disks driven by an electric motor could be chosen in the range 1 to 10 s^{-1}. The cavity was filled with the solution of glycerin in water ($\nu = 0.01$–0.05 cm^2/s). The typical value of the Ekman and Stewartson numbers was of the order 10^{-3}. Note that in preceding studies E was an order or two less and St an order or two greater.

All measurements were made with a DANTEC laser Doppler anemometer (LDA). Counter processor 55L90a provided accuracy of measurement of about 1.5% or better. The data from the LDA were processed in a personal computer. Radial and azimuthal velocity components were measured separately in the horizontal symmetry plane at the radius $r = (0.2\text{–}0.9)R$. No measurements were made beyond the symmetry plane. Account of the laser beam refraction at curved walls of the vessel was taken in processing experimental data.

The influence of the non-rotating sidewall is restricted to the region $r > R-H$ when disks are rotating at a constant angular velocity (Dolzhanskii & Krymov 1985). Beyond this region the fluid is in solid-body rotation, which was verified by independently measuring angular velocities of the fluid and disks.

3. Self-similar spin-down to rest

The theoretical solution found in K&M(*a*) for the case of quasi-solid-body-rotation spin-down to rest between infinite disks, is of the form (in dimensional variables)

$$u = \frac{r}{t+t_0}, \quad v = \frac{H^2}{\nu h_0^2}\frac{r}{(t+t_0)^2}, \quad w = \frac{-2z}{t+t_0}, \tag{3}$$

where

$$t_0 = \frac{H}{\alpha_0(\Omega\nu)^{\frac{1}{2}}}$$

is defined by the initial rotation rate Ω, ν is the fluid viscosity, H is the distance between disks, (u, v, w) are the velocity components in the cylindrical coordinate system (r, ϕ, z) and $\alpha_0 = 1.369$ is the dimensionless Ekman suction parameter calculated for the Kármán single-disk problem by Rogers & Lance (1960). Their results are relevant for our problem, because the solution (3) was obtained by matching internal and boundary-layer asymptotics, boundary-layer equations being the stationary Kármán equations for the single-disk problem. This is also the case for the conical geometry of Dolzhanskii (1985) and K&M(*b*).

The corresponding experimental data obtained in a low cylinder are represented in figure 2 in the form of the time dependence of the quantity $\Theta = H/(\omega(t)\,\nu)^{\frac{1}{2}}$. According to (3), this dependence should be linear (the straight line in figure 2). This figure demonstrates good agreement between theoretical and experimental results. The value $\alpha_0 = 1.37 \pm 0.02$ calculated from experimental data for various Ω using least squares corresponds very well to that obtained by Rogers & Lance (1960) numerically. Figure 3 demonstrates the theoretical and experimental dependencies of radial velocity (dimensional) on time. Though the inertial oscillations play an essential role, the theoretical curve correctly describes the average behaviour of $u(t)$.

It should be noted that this theory works if the Ekman number is less than about 0.02. On the other hand, when E is greater than this value the linear theory (Dolzhanskii & Krymov 1985) is applicable. This is confirmed by experimental data.

The full system of equations for the internal region and boundary layers coupled via Ekman suction was found in K&M(*a*) to admit a one-parameter family of self-similar substitutions, which unify time and radius dependence through a single variable $\xi = rt^{2/(p-1)}$ ($p > 0$ is the parameter). The two asymptotic forms of such self-similar solutions represent (i) the power-law initial state $v_0 = Ar^p$ and (ii) the unique quasi-solid-rotation stage given by (3) with $t_0 = 0$. The latter occupies the domain $r \gg t^{2/(1-p)}$ when $p > 1$ and $r \ll t^{2/(1-p)}$ when $p < 1$, which shows that it widens with

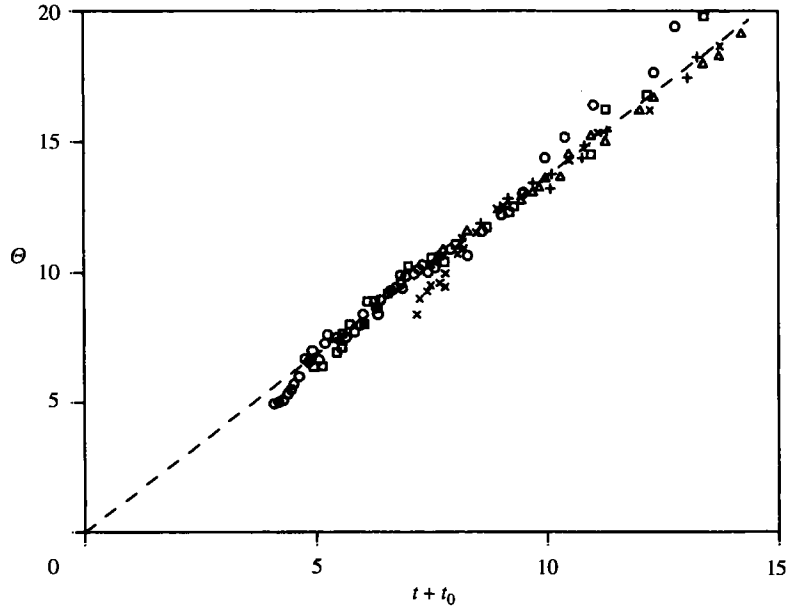

FIGURE 2. The dependence of the dimensionless quantity $\Theta = H/(\omega\nu)^{\frac{1}{2}}$ on shifted dimensionless time $t+t_0$: ---, formula (3); points – experiment at Ekman number: ○, 6×10^{-4}; □, 1×10^{-3}; △, 1.4×10^{-3}; +, 1.7×10^{-3}; ×, 1.8×10^{-3} (at radius $r = \frac{1}{2}R$).

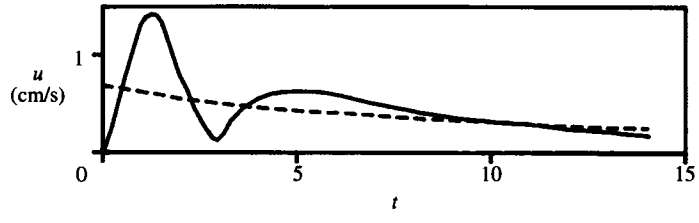

FIGURE 3. The radial velocity at radius $r = \frac{1}{2}R$ during spin-down *vs.* time: ——, experiment; ---, theory (3).

time. This can be understood if we notice that the fluid 'forgets' its initial state when t is significantly greater than t_0 (cf. (3)).

This was experimentally confirmed in K & M (*b*) for spin-down in the space between two cones: $|z| < r\cot\theta_0$. Such a configuration was first considered by Dolzhanskii (1985), who demonstrated that boundary layers on conical surfaces and on disks are governed by the same Kármán equations. Accordingly, the spin-down is qualitatively similar in these two cases, but the final stage of spin-down between cones is characterized by another radial dependence: $v \propto r^3/\nu t^2$. So if the initial state is the solid rotation, one can expect to observe the cubic dependence on r at large t.

The self-similarity of spin-down between cones is demonstrated in figure 4, where the dimensionless angular velocity ω/Ω (this quantity will be denoted from here on as ω) is plotted *vs.* the self-similar coordinate $\xi = r/t(\Omega\nu)^{\frac{1}{2}}$ (the special case of $p = 1$, solid rotation initial state). The final stage with $\omega \propto r^2$ is shown in figure 5.

Let us now test the Wedemeyer approximation for spin-down. The dimensionless Ekman suction condition in this case takes the form

$$u = \kappa\nu^{\frac{1}{2}}r^{\frac{1}{2}}E^{\frac{1}{2}}$$

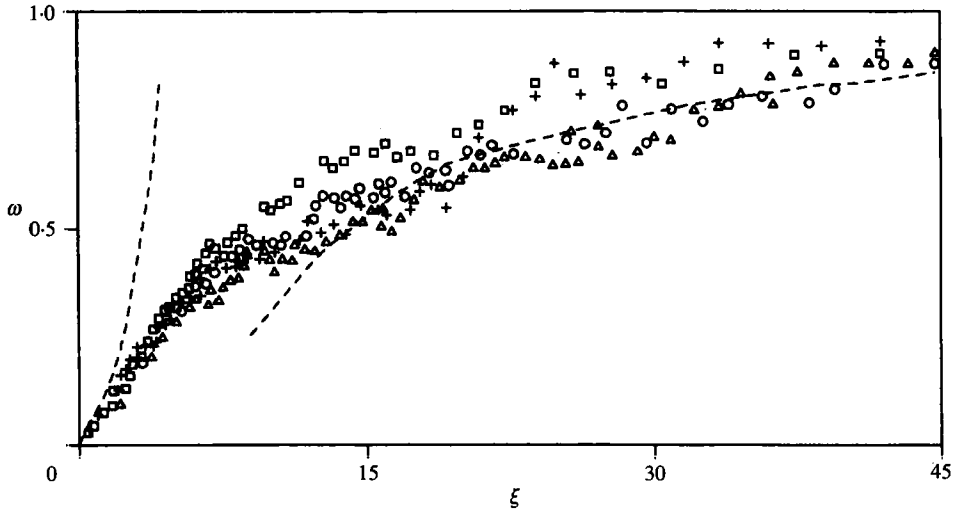

FIGURE 4. The dimensionless angular velocity ω during spin-down between cones plotted *vs.* the self-similar variable $\xi = r/t(\Omega\nu)^{\frac{1}{2}}$. Dashed curves correspond to asymptotic solutions; experimental points are obtained at: ○, $r = 0.45$, $\Omega = 2.5\ \mathrm{s}^{-1}$; □, $r = 0.45$, $\Omega = 11.3\ \mathrm{s}^{-1}$; △, $r = 0.56$, $\Omega = 2.6\ \mathrm{s}^{-1}$; +, $r = 0.6$, $\Omega = 8.9\ \mathrm{s}^{-1}$.

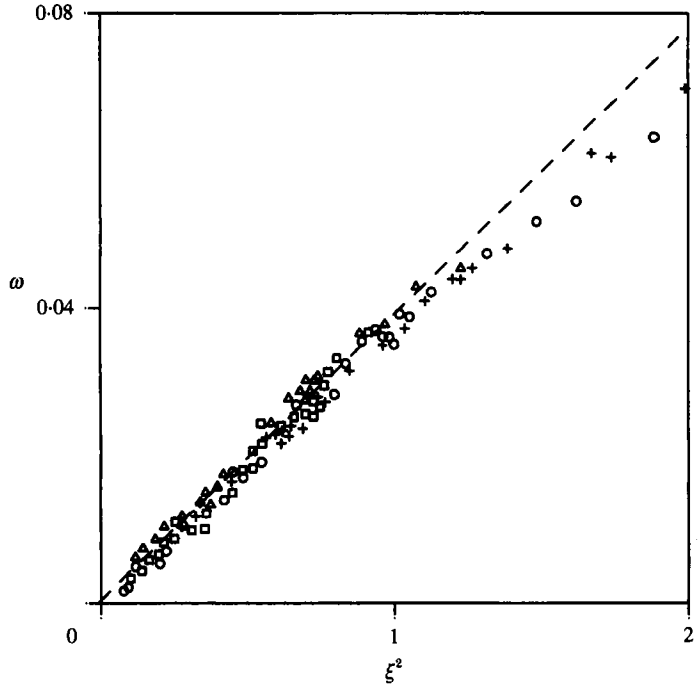

FIGURE 5. Same as in figure 4, but *vs.* ξ^2 and for smaller ξ-values. The long-time asymptotic is the dashed line; experimental points are obtained at: ○, $r = 0.38$, $\Omega = 13.9\ \mathrm{s}^{-1}$; □, $r = 0.38$, $\Omega = 15.5\ \mathrm{s}^{-1}$; △, $r = 0.56$, $\Omega = 12.2\ \mathrm{s}^{-1}$; +, $r = 0.56$, $\Omega = 15.7\ \mathrm{s}^{-1}$.

(velocity is normalized here by ΩR, Ω being the initial angular velocity of the container). So instead of (1) we have

$$\frac{\partial v}{\partial t}+\kappa^{\frac{1}{3}}r^{\frac{1}{3}}\left(\frac{\partial v}{\partial r}+\frac{v}{r}\right)=0$$

(viscous term is neglected). It is readily seen that there is a solution identical to (3) with $\alpha_0=\kappa$. The theoretical value $\alpha_0=1.369$ is confirmed by experimental data, so $\kappa=1.369$ should be taken. This equation also admits the self-similar substitution

$$v=t^{-2p/(p-1)}g(\xi),\quad \xi=rt^{2/(p-1)}$$

($p>0$ is a parameter) which leads to an ordinary differential equation for $g(\xi)$:

$$\frac{\mathrm{d}g}{\mathrm{d}\xi}=-\frac{g}{\xi}\frac{-2p\xi^{\frac{1}{3}}+(p-1)\kappa g^{\frac{1}{3}}}{2\xi^{\frac{1}{3}}+(p-1)\kappa g^{\frac{1}{3}}}.$$

This gives an asymptotic form $g\sim\text{const}\times\xi^p$, or $v\sim\text{const}\times r^p$, valid at large ξ if $p>1$ and at small ξ if $p<1$, i.e. at $t\to 0$. Thus, these solutions correspond to power-law initial conditions. The asymptotic form at $t\to\infty$ is given by $g\sim\xi/\kappa^2$, or $v\sim r/\kappa^2t^2$, which is again the quasi-solid-body spin-down to rest.

From the above analysis it follows that the Wedemeyer approximation correctly describes the principal qualitative features of self-similar spin-down. However, to achieve quantitative agreement one should be careful about the value of κ, which can vary if non-solid-body rotation is present (see K&M). Taking this all into account, we proceed now to the spin-up problem.

4. The general-form solution of the Wedemeyer equation for spin-up

Recall that the inviscid Wedemeyer equation

$$\frac{\partial v}{\partial t}+\kappa(v-r)\left(\frac{\partial v}{\partial r}+\frac{v}{r}\right)=0 \tag{4}$$

has the solution found by Wedemeyer

$$v=0 \qquad (r\leqslant \mathrm{e}^{-\kappa t}), \tag{5a}$$

$$v=\frac{r\,\mathrm{e}^{2\kappa t}-1/r}{\mathrm{e}^{2\kappa t}-1} \qquad (r\geqslant \mathrm{e}^{-\kappa t}). \tag{5b}$$

However, a general-form solution satisfying arbitrary initial conditions can be obtained.

First, rewrite (4) in terms of angular velocity $\omega=v/r$:

$$\omega_t-\kappa(1-\omega)(2\omega+r\omega_r)=0$$

(indices denote derivatives). Now let ω and r be independent variables, and let us seek the solution $t=t(\omega,r)$. Upon substituting $\omega_t=1/t_\omega$ and $\omega_r=-t_r/t_\omega$ we obtain

$$1-\kappa(1-\omega)(2\omega t_\omega-rt_r)=0.$$

Next, denote $\xi=\ln\omega, \rho=\ln r$. This leads to

$$1-\kappa(1-\mathrm{e}^{\xi})(2t_\xi-t_\rho)=0.$$

Introducing a 'moving' coordinate $\zeta = \xi + 2\rho$, we get an ordinary differential equation:

$$1 - 2\kappa(1 - e^{\xi}) t_{\xi} = 0, \quad t = t(\xi, \zeta). \tag{6}$$

This equation has an obvious general-form solution

$$t = F(\zeta) - \frac{1}{2\kappa} \ln (e^{-\xi} - 1), \tag{7}$$

where F is an arbitrary function defined by the initial conditions. In fact, (7) can be rewritten in terms of the original variables:

$$2\kappa t = \ln T(\omega r^2) - \ln\left(\frac{1}{\omega} - 1\right), \quad \left(\frac{1}{2\kappa} \ln T(\omega r^2) = F \ln \omega r^2\right)$$

(the arbitrary function is redefined here), or in the final form

$$e^{2\kappa t} = \frac{\omega}{1 - \omega} T(\omega r^2). \tag{8}$$

Now at $t = 0$ we have $\omega = \omega_0(r)$, which defines the function T. Consider for example the case $\omega_0(r) = 0$ at $r < 1$ and 1 at $r > 1$. Then, evidently, $x \equiv \omega r^2 = 0$ at $r < 1$, ω at $r = 1$ and r^2 at $r > 1$. From (8) it follows that $T(x) = (1 - \omega_0)/\omega_0$, hence $T(x) = (1 - x)/x$ at $x < 1$, and $T(x) = 0$ at $x > 1$. This gives a solution in the form $e^{2\kappa t} = (1 - \omega r^2)/r^2(1 - \omega)$, equivalent to the Wedemeyer solution (5).

An important class of solutions is obtained from (8) as a special case $T(x) = x^{\alpha}$. This yields

$$t - \frac{\alpha}{\kappa} \ln r = \frac{1}{2\kappa} \ln \frac{\omega^{\alpha+1}}{1 - \omega}. \tag{9}$$

Evidently, these are self-similar solutions, namely travelling waves which preserve their shape in the coordinates $(\ln r, t)$. The asymptotic behaviour of (9) at $r \to 0$, $t = 1$ is $\omega \sim r^{-2\alpha/(1+\alpha)}$, which requires $-1 < \alpha < 0$. At $r \to \infty, t = 1$ we have from (9) $\omega \sim t - r^{2\alpha}$.

The importance of travelling-wave solutions (9) is due to the fact that they serve as asymptotic forms for a wide class of solutions. In fact, let the initial state $\omega_0(r)|_{t=0}$ satisfy the condition $\omega_0 \sim r^{-2\alpha/(1+\alpha)}$ when $r \to 0$. If we denote $x = \omega_0 r^2 \ll 1$, then at $x \to 0$ we get $x \sim r^{2/(\alpha+1)}$, $\omega_0 \sim x^{-\alpha}$ and $T(x) \sim x^{\alpha}$, which leads to (9). Note that this asymptotic is valid for non-small values of ω; the only requirement is that ωr^2 should be small.

The above argument cannot be directly applied to an experimental situation because of the dependence of the asymptotic solution on subtle details of the initial state, namely the angular velocity distribution at small radius values. Nevertheless it suggests analysis of the experimental results in an attempt to recognize the travelling wave solutions (9) as a universal stage of the spin-up process. In other words, we hope that every experimental run should demonstrate one of solutions (9) with specific values of α and κ, possibly dependent on the initial state.

5. Experimental results

As was pointed out above, the angular velocity of the fluid during spin-up was measured. The experimentally measured dependence of dimensionless angular velocity ω on dimensionless time t at different values of radius r is presented in figure 6. Corresponding parameter values are $E = 2 \times 10^{-3}$, $St = 2.8 \times 10^{-4}$. The initial stage

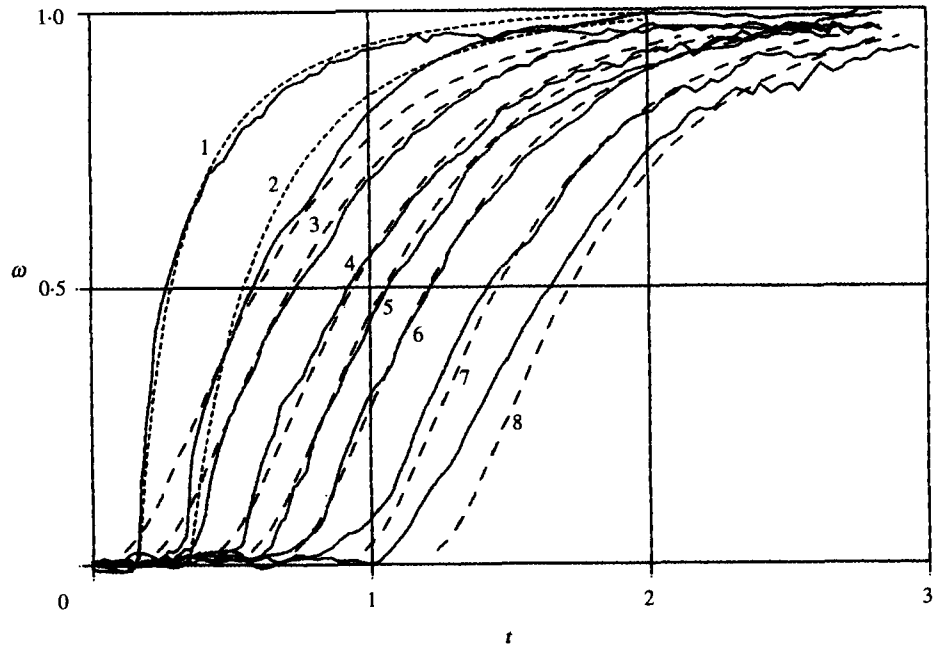

FIGURE 6. The dimensionless ω *vs* time for spin-up: ——, Experimental data at $E = 0.002$, $St = 2.8 \times 10^{-4}$ for $r = 0.86$, 0.71, 0.64, 0.5, 0.44, 0.37, 0.28, 0.21 (curves 1–8 respectively); – – –, travelling-wave solution (9); - - - -, Wedemeyer solution (5).

of spin-up (curves 1, $r = 0.86$) is well described by the Wedemeyer solution (short-dashed curve). At smaller radii the Wedemeyer solution fails (curves 2, $r = 0.71$). From here on, as r decreases, experimental curves approach one of the travelling-wave solutions (9), plotted in figure 6 by long-dashed curves.

Recall that these solutions depend on two parameters, the Ekman suction coefficient κ and the 'propagation velocity' $c = \kappa/\alpha$. Note that κ should be about unity (see Greenspan 1968), while the only *a priori* bound on c is $c < -\kappa$. The values of κ and c were found in the following manner. First, the arrival time T of the spin-up front at a certain radius was plotted *vs.* $\ln r$ as shown in figure 7. We considered the front position as the position of the inflexion point in the $\omega(t)$ dependence. From figure 6 one can estimate that the accuracy of the front position thus determined is not worse than 10%.

It is seen that the front propagates at a constant velocity (in $(t, \ln r)$ coordinates) nearly independent of external parameters in a certain range of E and St (experimental runs 2–4 in figure 7 represent only a part of all the experimental data used to determine c and κ). The velocity was taken as $c = -1.1$. Then, c given, the valuc of κ was chosen so that theoretical curves (9) would fit the corresponding experimental curves best. This procedure gives $\kappa = 1.0$ for all pairs (E, St) within the above-mentioned range which, oddly enough, is the value taken by Greenspan a few decades ago, see Greenspan (1968, p. 167). Thus, the class of solutions (9) is actually observed, and moreover, c and κ values are unique and independent of the initial state. For run 1 ($E = 0.0024$) the velocity c substantially increases at small r, and for $E > 0.0025$ the front propagation velocity is no longer more constant. The deviation of points in figure 7 (run 1) from a straight line exceeds the possible error in front position. The effect of non-small E and St is discussed below.

Let us now take a closer view at figure 6. It can be seen that the departure of the

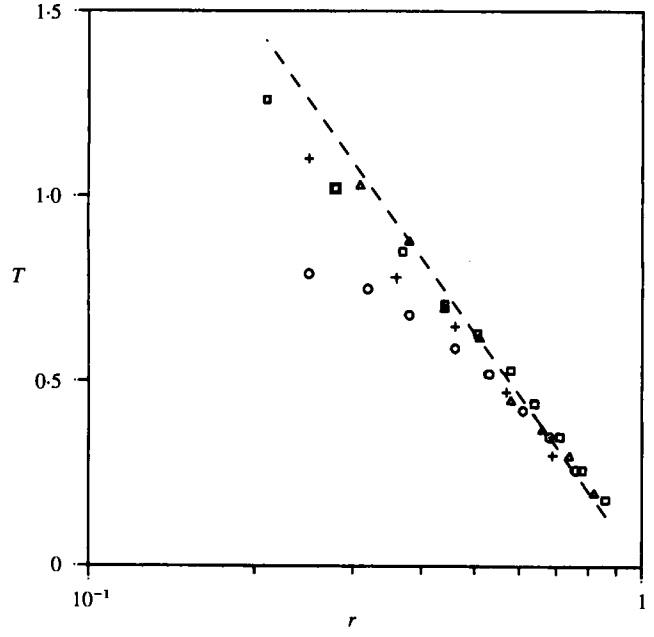

FIGURE 7. The arrival time of the front *vs.* radius (in log scale) at: ○, $E = 2.4 \times 10^{-3}$, $St = 1.8 \times 10^{-3}$; □, $E = 2.0 \times 10^{-3}$, $St = 2.8 \times 10^{-4}$; △, $E = 5.2 \times 10^{-4}$, $St = 5.5 \times 10^{-4}$; +, $E = 6.0 \times 10^{-4}$, $St = 5.0 \times 10^{-4}$; ---, exponential dependence on dimensionless 'front velocity' $c = -1.1$.

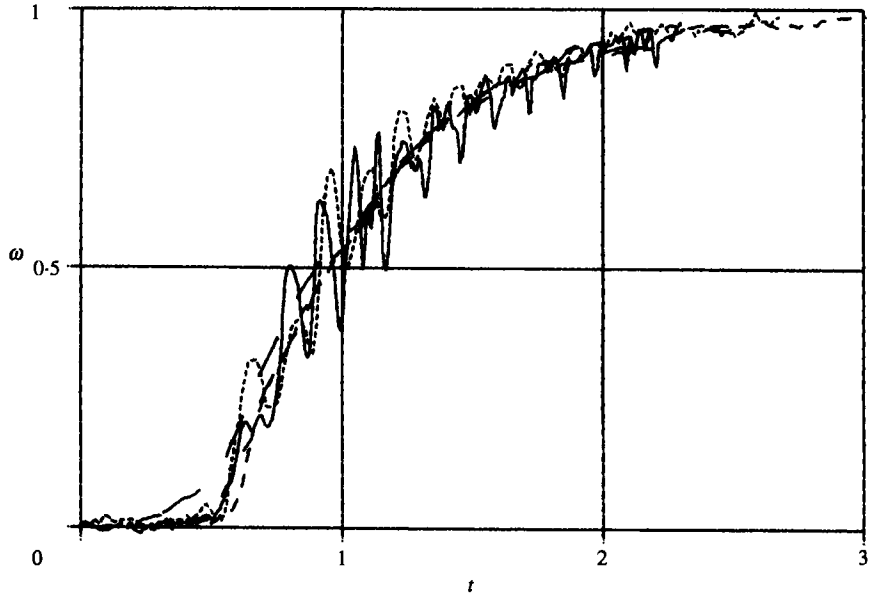

FIGURE 8. Experimental curves $\omega(t)$ shifted in time to demonstrate the uniqueness of their shape: ——, $E = 3 \times 10^{-4}$, $St = 7 \times 10^{-4}$, $r = 0.61$; ----, $E = 6 \times 10^{-4}$, $St = 5 \times 10^{-4}$, $r = 0.44$; ----, ---, ——, $E = 2 \times 10^{-3}$, $St = 2.8 \times 10^{-4}$, $r = 0.64$; 0.44; 0.28.

experimental curves from the Wedemeyer solution and their approach to the travelling-wave solution with $c = -1.1$, $\kappa = 1.0$ proceeds from high to low values of ω when radius decreases. At $0.3 < r < 0.5$ the agreement is good. Figure 8 demonstrates the uniqueness of the shape of the $\omega(t)$ dependence in the self-similarity

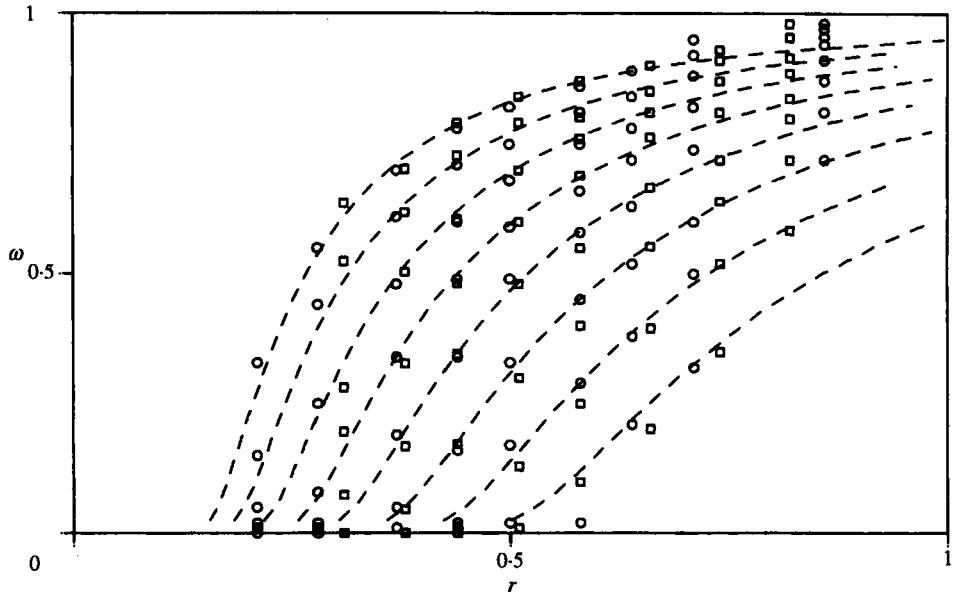

FIGURE 9. Dimensionless ω *vs.* r for $t = 0.45, 0.6, 0.75, 0.9, 1.05, 1.2, 1.35, 1.5$. Curves – theory (9), points – experiment with ○, $E = 2\times10^{-3}$, $St = 2.8\times10^{-4}$; □, $E = 6\times10^{-4}$, $St = 5\times10^{-4}$.

range for different values of E, St and r. All curves are shifted in t so that they can be compared directly. The theoretical curve is also plotted in this figure. The oscillations occurring at $E < 10^{-3}$ (figure 8) can be associated with a weak breakdown of the axial symmetry of the spin-up front. Their frequency is Ω and the amplitude grows with decreasing E. However, these oscillations have no effect on the average behaviour of $\omega(t)$.

Figure 7 shows that at small radius values ($r < 0.3$) the front propagation velocity slightly increases. Accordingly, experimental curves depart from theoretical ones. This is connected with the effect of viscosity. In order to demonstrate it more clearly, in figure 9 the radial dependence of ω is plotted for different t (two experimental runs: $E = 6\times10^{-4}$, $St = 5\times10^{-4}$ and $E = 2\times10^{-3}$, $St = 2.8\times10^{-4}$). Figure 9 shows that the front becomes steeper, i.e. its width decreases. Theoretical dashed curves approximate experimental points rather well and it can be seen that the front width at $t = 1.5$ is of the order 0.1. When it becomes comparable to the characteristic Stewartson layer width the inviscid approximation is no longer valid. Note also that the considerable width of the front supports the assumption of the local Kármánian structure of end-wall boundary layers.

6. Viscous spin-up

In this section we briefly describe another limiting case, namely when E is relatively large and the fluid acceleration occurs principally because of the friction between horizontal fluid layers. Evidently in this case the angular velocity should be independent of radius beyond the vicinity of the sidewall. In fact, figure 10 demonstrates the uniqueness of the temporal dependence of the angular velocity for different values of r, H, ν. Note that the time is now scaled by the characteristic *viscous* time $\tau_\nu = H^2/\nu$. Only for $r = 0.88$ is a Wedemeyer-like curve observed. Other curves can be approximated (for $0.1 < \omega < 0.9$) by an exponential function $\omega = 1-\exp(\gamma(t_0-t))$, $\gamma \approx 15$, $t_0 \approx 0.034$.

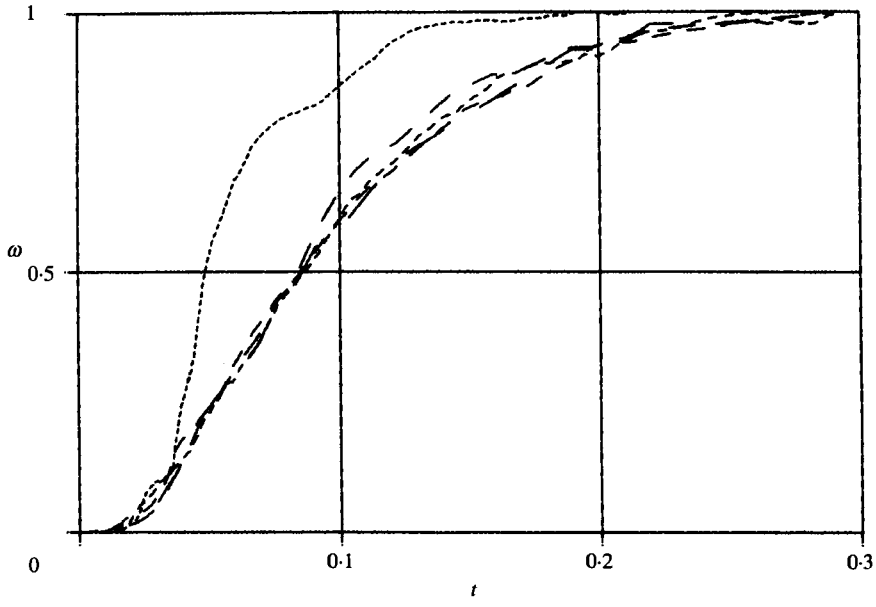

FIGURE 10. Experimental dependences $\omega(t)$ for viscous spin-up (time here is not shifted). Parameters: 1–3, $\nu = 0.01$ cm^2/s, $\Omega = 0.9$ s^{-1}, $h = 0.8$ cm ($E = 0.017$, $St = 0.0008$) at $r = 0.88$, 0.57, 0.43; 4–5, $\nu = 0.035$ cm^2/s, $\Omega = 0.9$ s^{-1}, $h = 1.5$ cm ($E = 0.016$, $St = 0.03$) at $r = 0.66$, 0.46.

For large E values spin-up and spin-down are completely equivalent. The corresponding theory was constructed by Dolzhanskii & Krymov (1985) including a simple formula for meridional circulation. It is valid for E less than about 0.025 and yields $\gamma \approx 10$. This value was also obtained experimentally by Dolzhanskii & Krymov (1985). The difference from $\gamma \approx 15$ found in this work is probably due to the fact that $E = 0.017$ is not large enough for the theory to be fully valid.

7. Conclusions

Summarizing the results of this and previous investigations we plot the experimental conditions in figure 11 in a $(\ln St, \ln E)$-plane. The horizontal dotted line marks the value $E = 0.0025$, found in this work to be the upper bound for essentially inviscid vertical momentum transfer. With $E > 0.0025$ the propagation of the front speeds up owing to the vertical momentum diffusion which comes into effect with increasing E (see figure 10).

The Stewartson number characterizes the horizontal momentum diffusion in the same way as E characterizes the vertical momentum diffusion. The vertical dotted line in figure 11 marks another upper bound, $St = 0.001$, for radially self-similar spin-up. The effect of the Stewartson number can be seen in figure 12, similar to figure 7 of Hyun *et al.* (1983). It shows that the front arrival time approaches its limiting value when $St < 0.001$.

The following principal results are obtained in the present work.

(i) The applicability of the Wedemeyer model to strongly nonlinear spin-up and spin-down is demonstrated via comparison with analytical results of asymptotic theory (spin-down) and experimental data (both spin-up and spin-down). The applicability domain of the Wedemeyer approximation in the plane of the governing parameters E and St is estimated.

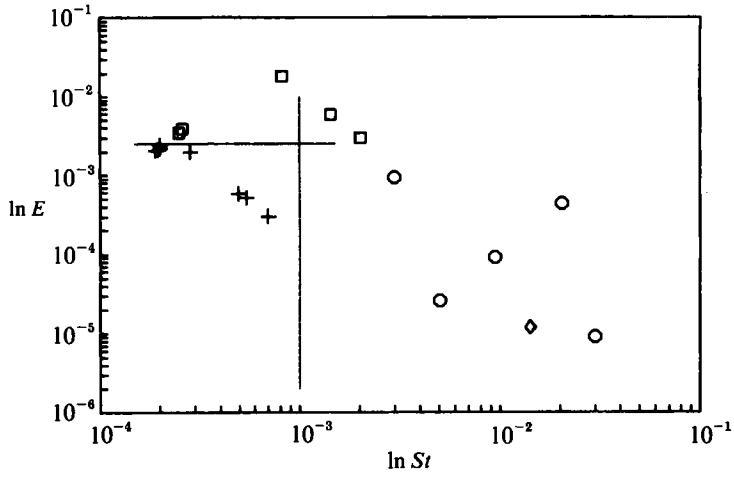

FIGURE 11. The experimental conditions for various experiments: ○, Hyun *et al.* (1983); ◇, Savaş (1985); □, this work, viscous and non-self-similar spin-up; +, this work, self-similar spin-up.

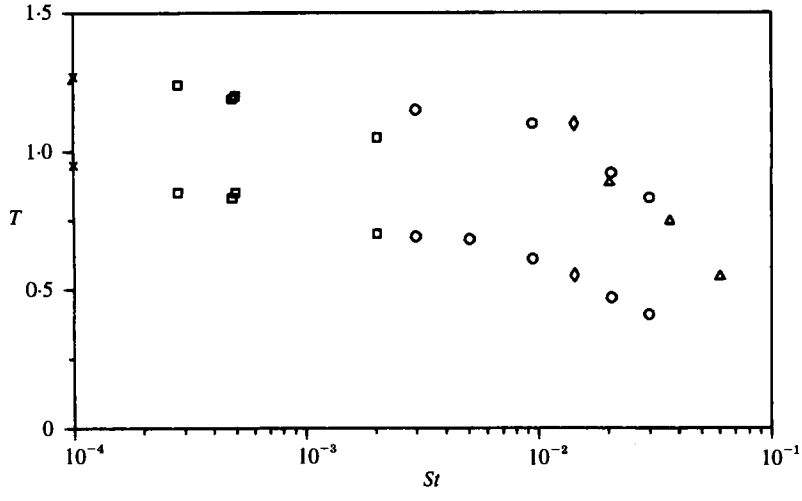

FIGURE 12. The time of front arrival (lower points) and the time for ω to reach $\frac{1}{2}$ (upper points) at radius $r = 0.39$ as functions of St: ○, Hyun *et al.* (1983); △, Watkins & Hussey (1977); ◇, Savaş (1985); □, this work; ×, Wedemeyer solution (5).

(ii) An exact solution of the initial-value problem for the Wedemeyer equation is found in an implicit form.

(iii) Detailed characteristics of the spin-up from rest are obtained experimentally. It is shown that the final stage of spin-up is described by a unique self-similar solution of the type (9) (propagating-wave solutions) with parameter values independent of initial conditions and external parameters (aspect ratio, Ω, H) in the applicability domain of the Wedemeyer equation. Another limiting case (relatively large Ekman number) is also examined.

(iv) There is no explanation for the specific value of the front propagation velocity $c = -1.1$ observed in this work. Though it is close to the limiting value $c = -\kappa = -1.0$, the difference is significant. (Otherwise the form of $\omega(t)$ curves would be Wedemeyer-like.)

REFERENCES

BENTON, E. R. 1973 Non-linear hydrodynamic and hydromagnetic spin-up driven by Ekman–Hartmann boundary layers. *J. Fluid Mech.* **57**, 337–360.

BENTON, E. R. 1979 Vorticity dynamics in spin-up from rest. *Phys. Fluids* **22**, 1250–1251.

DOLZHANSKII, F. V. 1985 Motion of a fluid between rotating cones. *Izv. Akad. Nauk SSSR, Mekh. Zhidk. Gaza* No. 2, 58.

DOLZHANSKII, F. V. & KRYMOV, V. A. 1985 Spin-down of a fluid in a low cylinder. *Izv. Akad. Nauk SSSR, Mekh. Zhidk. Gaza* No. 1, 19.

GREENSPAN, H. P. 1968 *The Theory of Rotating Fluids.* Cambridge University Press.

GREENSPAN, H. P. & HOWARD, L. N. 1963 On a time-dependent motion of a rotating fluid. *J. Fluid Mech.* **17**, 385–404.

GREENSPAN, H. P. & WEINBAUM, S. 1963 On non-linear spin-up of a rotating fluid. *J. Math. Phys.* **44**, 66–85.

HYUN, J. M., LESLIE, F., FOWLIS, W. W. & WARN-VARNAS, A. 1983 Numerical solutions for spin-up from rest in a cylinder. *J. Fluid Mech.* **127**, 263–281.

KITCHEN, C. W. 1980 Navier–Stokes solutions for spin-up in a filled cylinder. *AIAA J.* **18**, 929.

KRYMOV, V. A. & MANIN, D. YU. 1986*a* Spin-down of a fluid in a low cylinder at large Reynolds numbers. *Izv. Akad. Nauk SSSR, Mekh. Zhidk. Gaza* No. 3, 39–46 (referred to herein as K&M*a*).

KRYMOV, V. A. & MANIN, D. YU. 1986*b* Spin-down of a fluid between infinite cones. *Izv. Akad. Nauk SSSR, Mekh. Zhidk. Gaza* No. 4, 37–44 (referred to herein as K&M*b*).

MATHIS, D. M. & NEITZEL, G. P. 1985 Experiments on impulsive spin-down to rest. *Phys. Fluids* **28**, 449–455.

PROUDMAN, I. 1956 The almost-rigid rotation of viscous fluid between concentric spheres. *J. Fluid Mech.* **1**, 505–516.

ROGERS, M. H. & LANCE, G. N. 1960 The rotationally symmetric flow of a viscous fluid in the presence of an infinite rotating fluid. *J. Fluid Mech.* **7**, 617.

SAVAŞ, Ö. 1985 On flow visualization using reflective flakes. *J. Fluid Mech.* **152**, 235–248.

STEWARTSON, K. 1957 On almost rigid rotations. *J. Fluid Mech.* **3**, 17–26.

VENEZIAN, G. 1969 Spin-up of a contained fluid. *Topics in Ocean Engng* **1**, 212.

VENEZIAN, G. 1970 Nonlinear spin-up. *Topics in Ocean Engng* **2**, 87.

WATKINS, W. B. & HUSSEY, R. G. 1973 Spin-up from rest: limitations of the Wedemeyer model. *Phys. Fluids* **16**, 1530.

WATKINS, W. B. & HUSSEY, R. G. 1977 Spin-up from rest in a cylinder. *Phys. Fluids* **20**, 1596–1604.

WEDEMEYER, E. H. 1964 The unsteady flow within a spinning cylinder. *J. Fluid Mech.* **20**, 383–399.

WEIDMAN, P. D. 1976*a* On the spin-up and spin-down of a rotating fluid. Part 1. Extending the Wedemeyer model. *J. Fluid Mech.* **77**, 685–708.

WEIDMAN, P. D. 1976*b* On the spin-up and spin-down of a rotating fluid. Part 2. Measurements and stability. *J. Fluid Mech.* **77**, 709–735.